ESR spectroscopic characterization of V_2O_5/AlF_3 ammoxidation catalysts

K.V. Narayana [c], B. David Raju [a], S. Khaja Masthan [a], V. Venkat Rao [a],
P. Kanta Rao [a], R. Subrahmanian [b], A. Martin [c,*]

[a] *Catalysis and Physical Chemistry Division, Indian Institute of Chemical Technology, Hyderabad 500 007, India*
[b] *National Institute of Nutrition, Hyderabad 500 007, India*
[c] *Institut für Angewandte Chemie Berlin-Adlershof e.V.* [1], *Richard-Willstätter-Str. 12, D-12489 Berlin, Germany*

Abstract

Electron spin resonance (ESR) spectroscopic study has been made at 25 °C on a series of V_2O_5/AlF_3 catalysts, prepared by wet impregnation method with different V_2O_5 loadings ranging from 2 to 15 wt%. V_2O_5/AlF_3 solids have been used as catalysts in the ammoxidation of 3-picoline to nicotinonitrile. The ESR parameters like $g_\parallel$, $g_\perp$, $A_\parallel$, $A_\perp$ were obtained from the spectra from which isotropic g factor (g_0), isotropic hyperfine interaction factor (A_0) and bonding parameters (α^2, β_2^2, B, C, K) were calculated. The well-resolved ESR spectra of catalysts indicate the paramagnetic nature of V^{4+} (VO^{2+}) species on the AlF_3 support, which are in the distorted octahedral environment. The integral intensity of V^{4+} species and the selectivity to nicotinonitrile are increasing with increase in V_2O_5 loading, which may be due to facile redox mechanism (V^{4+}/V^{5+}) or the progressive increase in V^{4+} interaction along with V_2O_5 loading.
© 2004 Elsevier B.V. All rights reserved.

Keywords: V_2O_5/AlF_3 catalysts; ESR spectroscopy; Ammoxidation; 3-picoline; Nicotinonitrile

1. Introduction

Vanadium oxide supported on conventional carriers like Al_2O_3, SiO_2, TiO_2, ZrO_2 has been widely investigated by the electron spin resonance (ESR) spectroscopy [1–8]. ESR spectroscopy is a highly sensitive technique for the investigation of paramagnetic species having one or more unpaired electrons either in the bulk or at the surface of the catalytic materials, that reveals useful information about the catalyst regarding: (i) the local structure surrounding the V^{4+} ions, (ii) effect of carrier on the V^{4+} species, (iii) micro-structural changes either in the support or in the active component, and (iv) nature of the paramagnetic species that influence catalytic behavior. As reported by Ciambelli et al. [9], ESR spectroscopy is a powerful tool for the characterization of V^{4+} ions even in lower proportions (lower limit 1% of V^{4+} ions).

Vanadia catalysts supported on different carriers (Al_2O_3, SiO_2, ZrO_2, TiO_2, zeolites, mesoporous molecular sieves and modified clays) exhibit different catalytic properties depending on the physico-chemical properties of the support. The ESR study of Yoshida et al. [10] reported the presence of VO_x species on V_2O_5/γ-Al_2O_3 catalysts as square pyramidal VO_5 units. Recently, Nakajima [11] have also reported that the ESR parameters, $g_\parallel$ and $A_\parallel$ of VO^{2+} in the persimmon tannin gel indicated the square pyramidal coordination structure of VO^{2+} with hydroxy groups in catachol, pyrogallol and water. Tetragonal geometry of vanadium ions has been observed for impregnated V_2O_5/SiO_2 catalysts

---

carried out at high-vacuum treatment [12]. Cavani and Busca [6] reported that during V_2O_5/TiO_2 catalyst preparation by impregnation technique using aqueous solution of ammonium metavanadate, some reduction occurred; consequently superficial V^{4+} ions were generated, which were confirmed as isolated vanadyl species by ESR spectroscopy.

Nevertheless, substantial amount of study has not been made so far on fluoride supported vanadia catalysts in general, AlF_3 supported vanadium oxide system, in particular. AlF_3 is a novel and non-conventional support and we have found recently that V_2O_5/AlF_3 is an efficient catalyst for the ammoxidation of 3-picoline to nicotinonitrile [13]. The understanding of the catalytic behavior requires an appropriate evaluation of the vanadium species involved in the reaction. Hence, in the present study, AlF_3 supported vanadium oxide catalysts have been characterized by ESR spectroscopy for better understanding of the coordination environment of vanadium species.

2. Experimental

2.1. Catalyst preparation

V_2O_5/AlF_3 catalysts with V_2O_5 loading from 1.96 to 14.98 wt% were prepared by wet impregnation method using $AlF_3 \cdot 3H_2O$ (Aldrich) and NH_4VO_3 (Aldrich), respectively. Requisite amount of NH_4VO_3 was dissolved in an aqueous oxalic acid solution and impregnated by contacting the support particles. The excess solution was evaporated to dryness on a water bath. The catalyst samples were oven dried at 393 K for 16 h and calcined at 723 K for 6 h in air. The $AlF_3 \cdot 3H_2O$ yielded α-AlF_3 as a major phase with some traces of $AlF_{1.96}(OH)_{1.04}$ phase after calcination at 723 K for 6 h (i.e. after removal of crystalline water). AAS (Perkin–Elmer, Model: 2380) was used for the determination of vanadium contents of the catalysts.

2.2. ESR spectroscopic measurements

ESR spectra of V_2O_5/AlF_3 catalyst samples were recorded at 25 °C on a Bruker ER-200-SRC X-band spectrometer at a microwave frequency of 9.78 GHz and a modulation frequency of 100 kHz and calibrated with a 2,2-diphenyl-1-picrylhydrazyl hydrate (DPPH). All the samples were crushed in an agate mortar and a defined amount (ca. 20 mg) of the sample was dried overnight at 120 °C and then introduced into an ESR tube for analysis. The integral intensity of the V^{4+} signal was calculated as the product of the height of the signal and the square of the ΔH (peak to peak line width). The intensity values were normalized for instrumental factors like modulation and gain [14].

2.3. Catalytic activity

The ammoxidation reaction was carried out in a fixed bed glass reactor in the vapour phase at atmospheric pressure and a reaction temperature of 360 °C. The 3-picoline + H_2O mixture (1:2.5 v/v ratio) was fed to the reactor at a flow rate of 2 ml/h along with NH_3 and air. The molar ratios of 3-picoline:H_2O:NH_3:air are maintained at 1:13:6:44. The catalytic tests were performed over 2 g of catalyst admixed with glass beads as diluents. The product analysis was made by GC. The detailed experimentation has been reported elsewhere [13].

3. Results and discussion

The ESR spectrum of 1.96 wt% V_2O_5/AlF_3 catalyst was taken as an example for better description of the results (Fig. 1). The spectrum indicates the presence of V^{4+} ions, in the form of vanadyl (VO^{2+}) species. From this spectrum, the basic ESR parameters like $g_\parallel$, $g_\perp$, $A_\parallel$ and $A_\perp$ were calculated (h is the Planck's constant, v is the frequency of the spectrometer and β is the Bohr magneton).

$$H_\parallel(0) = hv/g_\parallel\beta \tag{1}$$

$$H_\perp(0) = hv/g_\perp\beta \tag{2}$$

Measurements for $H_\parallel$ position were taken, which correspond to a maximum in the first derivative curve of the parallel hyperfine structure component for a given m value (magnetic quantum number of the vanadium nucleus having the values $\pm7/2$, $\pm5/2$, $\pm3/2$, $\pm1/2$), whereas the $H_\perp$ position is enclosed between the first derivative perpendicular peak and its 'zero' value. $A_\parallel$ and $A_\perp$ are obtained from the spectrum (Fig. 1) by taking the seventh parts of the magnetic induction in the parallel and perpendicular range from $m = +7/2$ to $-7/2$, respectively.

The ESR spectra of bulk V_2O_5 and AlF_3 supported V_2O_5 catalysts are presented in Fig. 2. All the V_2O_5/AlF_3 catalysts exhibited well-resolved hyper fine spectra that can be clearly seen from spectra b–f (Fig. 2). As evidenced from the well documented literature, the unpaired electrons of V^{4+} ($3d^1$) interacts with the magnetic moment of the ^{51}V nuclei ($I = 7/2$, natural abundance 99.75%) causing the appearance of a spectrum composed of eight parallel and eight perpendicular lines of the hyperfine structure [15–17].

Despite the spectra recorded under similar conditions, the disappearance of hyperfine splitting lines of bulk V_2O_5 (spectrum a, Fig. 2) and appearance of hyperfine splitting lines of all the supported V_2O_5 catalysts (spectra b–f, Fig. 2) are in good agreement with literature reports [18–20]. Signal of bulk V_2O_5 (spectrum a, Fig. 2) at $g = 1.962$ is broad with peak-to-peak line
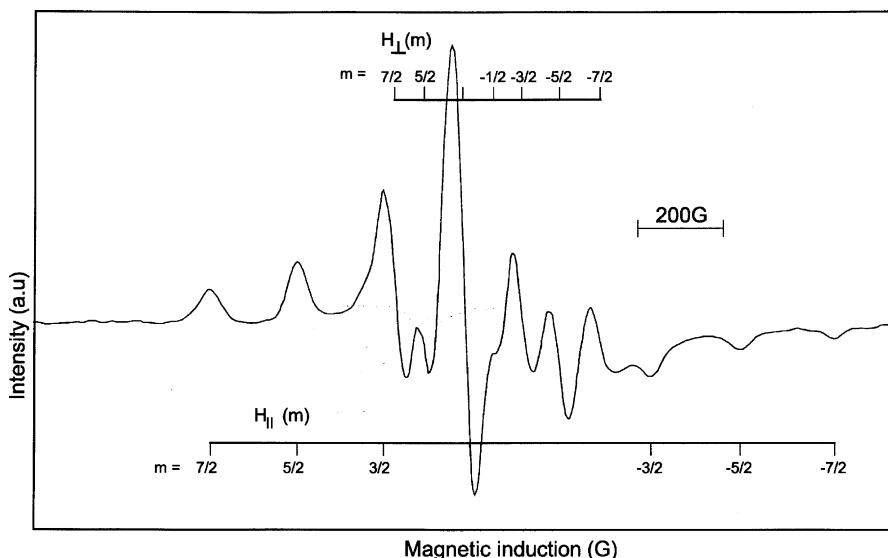
Fig. 1. ESR spectrum of 1.96 wt% V_2O_5/AlF_3 catalyst.

width of 110 G, which is typical for V^{4+} species. The absence of hyperfine structure indicates that the ions are subjected to relatively strong interactions suggesting that the signal is due to clustered V^{4+}, most likely immersed into an oxidic vanadium phase [17,18].

Spin-Hamiltonian parameters ($g_\parallel$, $g_\perp$, $A_\parallel$ and $A_\perp$) were determined from the intense peaks of the spectrum and the molecular orbital coefficients α^2 and β_2^2 (values are given in Table 1) were obtained from a suitable linear combination of the $g_\parallel$ and $g_\perp$, and also $A_\parallel$ and $A_\perp$, which are defined by the following equations [18,21].

$$\alpha^2 = 7/4[(A_\parallel - A_0)/P + 2/3g_\parallel - 5/21g_\perp - 6/7], \qquad (3)$$

where P is a term, which takes into account the dipole–dipole interaction of the electron moment with the nuclear moment. In the present work the value of $P = 184.5$ G obtained from [18] has been used, and A_0 is the isotropic hyperfine interaction factor obtained from the equation $A_0 = (A_\parallel + 2A_\perp)/3$ [22]. α^2 represents in-plane σ-bonding

$$\beta_2^2 = -7/6\Delta g_\parallel + 5/12\Delta g_\perp + 7/6[(A_\parallel - A_\perp)/P], \qquad (4)$$

where $\Delta g_\parallel = g_e - g_\parallel$, $\Delta g_\perp = g_e - g_\perp$, g_e indicates the free electron g value i.e., 2.0023. β_2^2 represents the axial ligand π-bonding. The values of β_2^2 are found to be almost same in all the cases, which indicate that the delocalization of electrons is not great and hence the π-bonding ability of the oxygen is very poor (see Table 1).

The isotropic or Fermi contact term K is represented by the following equation (see Table 1):

$$K = A_0/(P - \Delta g_0), \qquad (5)$$

where $\Delta g_0 = g_e - g_0$, g_0 is the isotropic g factor obtained from the equation $g_0 = (g_\parallel + 2g_\perp)/3$. From Eq. (5), it is clear that K is directly proportional to A_0. It indicates

the interaction between the electronic and the nuclear spins. K is an independent property of the central ion

$$C = 1 - \beta_2^2. \qquad (6)$$

The term C represents the fraction of delocalization of the unpaired d electrons over ligand orbitals. The values of C (see Table 1) indicate the delocalization, which observed to be remained same in all the loadings of V_2O_5 on AlF_3 support

$$B = \Delta g_\parallel / \Delta g_\perp. \qquad (7)$$

The term B indicates the extent of tetragonal distortion which relates to bond length or strength of both V double bond oxygen (V=O) and V single bond oxygen (V–O) ligand. The value of B (see Table 1) is also found to remain almost unchanged in all the V_2O_5/AlF_3 catalysts with different V_2O_5 loadings.

The values of $g_\parallel$, $g_\perp$ depend on the vanadium-ligand distance, increase of $g_\parallel$ and $g_\perp$ values cause shortening of V–O and V=O bond lengths, respectively, or vice versa [23]. The experimentally obtained g values are more or less constant at $g_\parallel = 1.93$ and $g_\perp = 1.96$ for all the catalysts (the same constant behavior is found for $A_\parallel$ and $A_\perp$, being 205 and 67 G, respectively). Abundant literature [19,24] on ESR spectroscopic studies on V_2O_5/Al_2O_3 catalysts reported the $g_\parallel = 1.92$–1.94 and $g_\perp = 1.97$–2.00, thus, our data are in good agreement with the reported literature [19].

$g_\perp > g_\parallel$ and $A_\parallel > A_\perp$, is the general trend for tetrahedral, square pyramidal, distorted octahedral and octahedral geometric environment of VO^{2+} ions [5]. In order to distinguish among the stated geometric environment A_0 and g_0 values are to be taken into consideration. The isotropic g-factor g_0 and the isotropic hyperfine interaction factor A_0 are estimated to be 1.95
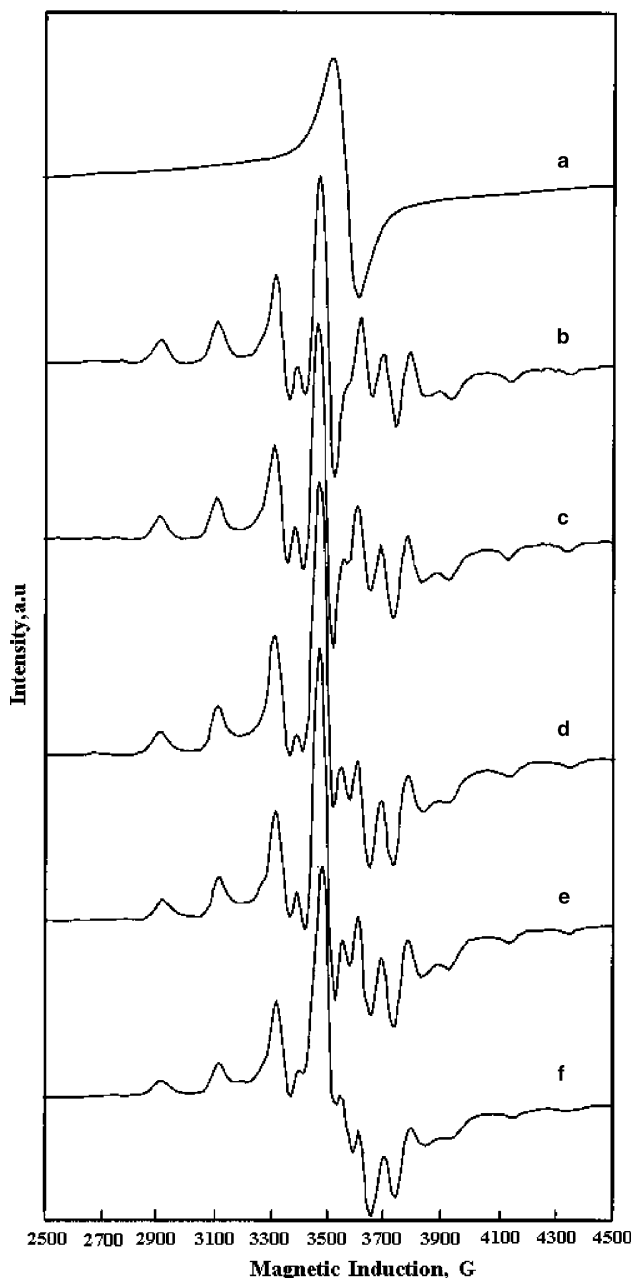
Fig. 2. ESR spectra of pure V_2O_5 and AlF_3 supported V_2O_5 catalysts with different V_2O_5 loadings: (a) pure V_2O_5; (b) 1.96 wt%; (c) 5.71 wt%; (d) 7.58 wt%; (e) 10.52 wt%; (f) 14.98 wt%).

Table 1
ESR Spin Hamiltonian parameters of V^{4+} in V_2O_5/AlF_3 catalysts: bonding coefficients and Fermi contact term values

Catalysts	α^2	β_2^2	K (G)	C	B
1.96%V_2O_5/AlF_3	0.807	0.805	0.622	0.195	1.65
5.71%V_2O_5/AlF_3	0.809	0.807	0.619	0.193	1.75
7.58%V_2O_5/AlF_3	0.813	0.811	0.619	0.189	1.71
10.52%V_2O_5/AlF_3	0.802	0.800	0.614	0.199	1.70
14.98%V_2O_5/AlF_3	0.807	0.806	0.619	0.195	1.70

pyramidal complexes. ESR spectra of axially distorted octahedral geometry is generally difficult to distinguish from that of square pyramidal geometry because the sixth ligand is weakly bonded to the trans position to the double bond (V=O) and only slightly modifies the unpaired electron distribution [5]. Our ESR spectroscopic results are in agreement with the literature reports regarding the local geometry of vanadium species deposited on Al_2O_3 [19], SiO_2 [25,26], MgO [27] and MgF_2 [20].

The squared molecular orbital coefficients, α^2 and β_2^2 are compiled in Table 1, are found to be constant at all the loadings of the used V_2O_5/AlF_3 catalysts. β_2^2 is a coefficient accounting for the participation of the d_{xy} atomic orbital in the anti-bonding orbital centered mainly on the cation of the vanadyl complex. This coefficient is associated with the electron delocalization on the cation [28]. Bahranowski et al. [29] reported that a material possessing lower values of the β_2^2 will have not only the higher delocalization of un paired electrons over the ligands but also higher degree of in-plane π-covalent bonding. The authors concluded that the electronic structure of the V(IV) species present in the material and the higher degree of delocalization of the unpaired electron on the vanadium d_{xy} orbital is responsible for the higher catalytic performance of the catalyst in the oxidative dehydrogenation of propane.

The values of C (see Table 1) indicate that the delocalization of unpaired d-electrons on the oxygen ligands is constant in all the studied V_2O_5/AlF_3 catalysts. The values of Fermi-contact term K show the electron density of unpaired electron at the ^{51}V nucleus, which is found to be more or less constant with changing V_2O_5 loadings on AlF_3 support. It has also been reported [30] that the value of Fermi-contact term, K, is less than 0.79 ($K < 0.79$) attributes the presence of hexa-coordinated geometry of the vanadium ions. As is evident from Table 1 that the K values are in the range from 0.614 to 0.622, which are less than 0.79, hence it may be attributed to the presence of (VO)$^{2+}$ species in the distorted octahedral environment.

The values of the parameter B are observed to be in the range of 1.65–1.75. According to Sharma et al. [15], for a paramagnetic complex in square pyramidal or te-

and 113 G, respectively, for all the studied catalysts. As reported in the literature [24], $g_0 = 1.95$–1.98, $A_0 = 80$–120 G and along with the relation ship of $g_\perp > g_\parallel$ and $A_\parallel > A_\perp$ represents the VO^{2+} ions are present either in square pyramidal or distorted octahedral geometric environment. It is well known that the vanadium complexes generally contain a vanadyl group (VO^{2+}) in which the vanadium ion is strongly bonded to the "yl" oxygen ion. Four ligands in the equatorial plane complete the coordination sphere of the square

tragonally distorted octahedral surrounding, B is a sensitive indicator of changes in the local symmetry. If no angular distortion occurs its increase points to either shortening of the V double bond oxygen (V=O) or the elongation of the distance to the in-plane ligands (in-plane V single bond oxygen V–O). It is reported that the B values are ranging from 3.0 to 5.0 in H-ZSM-5 zeolites, whereas on either silica or alumina, the values are ranging from 2.0 to 2.4. This is an indication of the high stability of VO^{2+} complex in H-ZSM-5 zeolite in contrast to that on silica or alumina which is more than two times less [23]. The lower values of B of V_2O_5 loaded on AlF_3 as depicted in Table 1 ($B = 1.65–1.75$) are attributed to the lower stability (stability of sixth ligand contributing from the support bonded to the trans position to the vanadyl double bond) of V=O double bond in VO^{2+} complex on AlF_3 support compared to literature data of H-ZSM-5 ($B = 3.0–5.0$) or silica and alumina ($B = 2.0–2.4$) supports.

Correlation between signal intensity of V^{4+} species and nicotinonitrile selectivity as a function of V_2O_5 loading is presented in Fig. 3. The integral signal intensity of V^{4+} species is observed to increase steadily with increase in V_2O_5 loading from 1.96 to 14.98 wt%. The selectivity of nicotinonitrile is also observed to increase with V_2O_5 loading in a similar manner as of integral signal intensity (Fig. 3). The V^{4+} species present in the catalyst may be influencing its catalytic activity towards higher conversions and selectivities by facilitating the redox mechanism or by the interaction of V^{4+} species with V_2O_5. However, it is an important observation that both the integral intensity of V^{4+} species and the ammoxidation activity of the catalysts increased progressively with V_2O_5 loading.
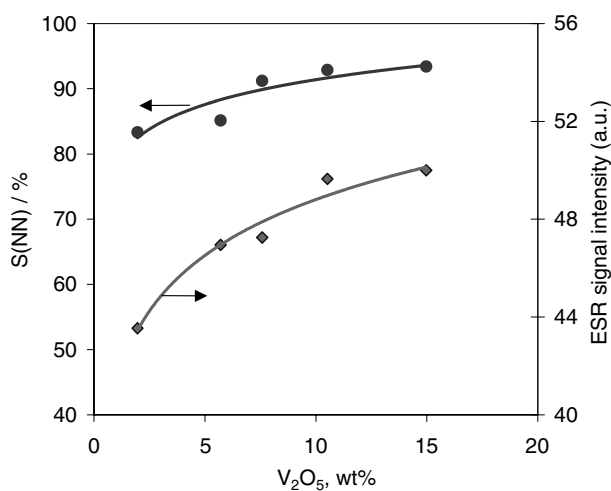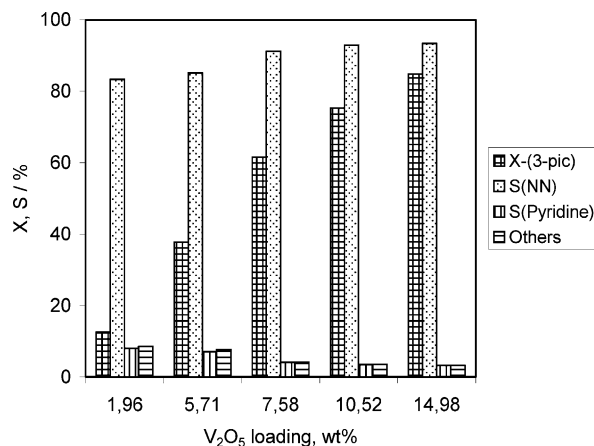

Fig. 4. Variation of catalytic activity with V_2O_5 loading on AlF_3 support.

The V_2O_5/AF_3 catalysts are proved to be active and selective catalysts for the present ammoxidation of 3-picoline to nicotinonitrile (Fig. 4). The selectivity of nicotinonitrile achieved is as high as 93% at 3-picoline conversion levels of ca. 85% under optimized reaction conditions ($T = 360$ °C, 3-picoline:H_2O:NH_3:air = 1:13:6:44 using 2 g catalyst) over 14.98 wt% V_2O_5/AlF_3 catalyst. It is evident from Fig. 4 that the conversion has continuously been increasing from 12% to 85% with increase in V_2O_5 loading from 1.96 to 14.98 wt%. The selectivity of nicotinonitrile is varied over a small range from 83% to 93% with varying V_2O_5 loadings. Pyridine and CO_x are the by-products of this ammoxidation reaction and also traces of 3-amidopyridine are observed in the product mixture. The production of pyridine and CO_x are mainly due to oxidative demethylation of 3-picoline and oxidative destruction of reaction intermediates, respectively. The enhancement in nicotinonitrile selectivity and the simultaneous diminishing in oxidative demethylated products selectivity may be attributed to the progressive interaction of vanadyl VO^{2+} species with increasing V_2O_5 loading.

4. Conclusions

The ESR spectra of V_2O_5/AlF_3 catalysts revealed the existence of V^{4+} species on the AlF_3 support. The results of the present investigation also indicate that the VO^{2+} ions are present in distorted octahedral environment. The similar increasing trend of integral intensity of V^{4+} species and the ammoxidation activity with V_2O_5 loading might be due to either facile redox (V^{4+}/V^{+5}) mechanism and/or increased V^{4+} species interaction. However, the progressive increase of V^{4+} species is the manifestation of the enhancement in the nicotinonitrile selectivity along with V_2O_5 loading on AlF_3 support for the selective 3-picoline ammoxidation.

Fig. 3. Correlation between V^{4+} species signal intensity and nicotinonitrile selectivity with V_2O_5 loading on AlF_3 (S(NN) = selectivity of nicotinonitrile).

References

[1] M. Inomata, K. Mori, A. Miyamoto, Y. Murakami, J. Phys. Chem. 87 (1983) 754.

[2] M. Niwa, Y. Murakami, J. Catal. 76 (1982) 9.

[3] M. Narayana, C.S. Narasimhan, L. Kevan, J. Catal. 79 (1983) 237.

[4] M. Che, J. Catal. 51 (1978) 143.

[5] A. Davidson, M. Che, J. Phys. Chem. 96 (1992) 9909.

[6] F. Cavani, G. Busca, Mater. Chem. Phys. 25 (1990) 475.

[7] M.J. Torralvo, M.A. Alario, J. Soria, J. Catal. 86 (1984) 473.

[8] A. Adamski, Z. Sojka, K. Dyrek, M. Che, Solid State Ionics 117 (1999) 113.

[9] P. Ciambelli, L. Lisi, G. Russo, J.C. Volta, Appl. Catal. B 7 (1995) 1.

[10] S. Yoshida, T. Iguchi, S. Ishida, K. Tarama, Bull. Chem. Soc. Jpn. 45 (1972) 376.

[11] A. Nakajiima, Talenta 52 (2002) 537.

[12] L.L. van Reijen, P. Cossee, Discus. Faraday Soc. 41 (1966) 277.

[13] K.V. Narayana, S.K. Masthan, V. Venkat Rao, B. David Raju, P. Kanta Rao, Catal. Commun. 3 (2002) 173.

[14] B. David Raju, K.S. Rama Rao, G.S. Salvapathi, P.S. Sai Prasad, P. Kanta Rao, Appl. Catal. A 209 (2001) 335.

[15] V.K. Sharma, A. Wokaun, A. Baiker, J. Phys. Chem. 90 (1986) 2715.

[16] K.V.R. Chary, B.M. Reddy, N.K. Nag, V.S. Subrahmaniam, C.S. Sunandana, J. Phys. Chem. 88 (1984) 2622.

[17] J. Haber, J. Stoch, M. Wojciechowska, Surf. Interface Anal. 15 (1990) 711.

[18] T. Blasco, L. Fernandez, A. Martinez-Arias, M. Sanchez-Sanchez, P. Concepcion, J.M.L. Nieto, Micropor. Mesopor. Mater. 39 (2000) 219.

[19] B.M. Weckhuysen, I.P. Vannijvel, R.A. Schoonheydt, Zeolites 15 (1995) 482.

[20] S. Gupta, N. Khanijo, A. Mansingh, J. Non-Cryst. Solids 181 (1995) 58.

[21] R. Niemann, D. Kievelson, J. Chem. Phys. 35 (1962) 149.

[22] J.A. Mc Millan, T. Halpern, J. Chem. Phys. 55 (1971) 33.

[23] D. Strugaru, E. Trif, V. Cristea, G. Gheorghe, R. Russu, Radiat. Phys. Chem. 45 (1995) 917.

[24] H. Ueda, Bull. Chem. Soc. Jpn. 52 (1979) 1905.

[25] G. Centi, S. Perathoner, F. Trifiro, A. Aboukais, C.F. Aissi, M. Guelton, J. Phys. Chem. 96 (1992) 2617.

[26] M. Che, B. Canosa, A.R. Gonzalez-Elipe, J. Phys. Chem. 90 (1986) 618.

[27] M. Inomata, K. Mori, A. Miyamoto, T. Ui, Y. Marakamski, J. Phys. Chem. 87 (1983) 761.

[28] D. Andreeva, T. Tabakova, L. Ilieva, A. Naydenov, D. Mehanjiev, M.V. Abrashev, Appl. Catal. A 209 (2001) 291.

[29] K. Bahranowski, R. Dula, F. Kooli, E.M. Serwicka, Colloids Surf. A 158 (1999) 129.

[30] O. Cozar, I. Ardelean, I. Bratu, S. Simon, C. Cracium, L. David, C. Cefan, J. Mol. Struct. 563-564 (2001) 421.